03.31.2024

JOURNAL OF

Health, Metabolism & Nutrition Studies (JHMNS) Vol. 3 No. 3

PHYSICO-CHEMICAL PROPERTIES OF POLYHEDRAL OLIGOMERIC SILESQUIOXANE COVALENT ORGANIC FRAMEWORKS FOR NAPROXEN ADSORPTION

BALA SULEIMAN; AND BUBA MOHAMMED

Department of Science Laboratory Technology, Federal Polytechnic Mubi (FPM), P.M.B, 35, Mubi, Adamawa State, Nigeria.

bsuleiman1983@gmail.com

Abstract

Covalent organic frameworks are porous crystalline compounds prepared from organic material bonded together by strong reversible covalent bonds that have a durable effect on the geometry arrangements and permeability. These substances are entirely made up of light elements like H, B, C, N, O, and Si. COF-S4, OAPS and 1,5-Dihydroxyanthraquionone (1,5-DHAQ), was successfully synthesized by condensation (solvothermal) via a Schiff base reaction ($R_1R_2C{=}NR'$), with a molar ratio of 1:8 for OAPS to linker, at a temperature 120 °C. The compound obtained was investigated using several

Introduction

Covalent organic frameworks (COFs) are a new type of nanoparticles that emphasizes on nanostructure precise arrangement into two-dimensional (2D) or three-dimensional (3D) structures (3D). This feature permits frameworks to be formed with great orderliness and the fine-tuning of the physicochemical system. Organic monomers are linked by strong covalent

E-ISSN 3026-8664 P-ISSN3027-2238

spectroscopic techniques, including PXRD, FTIR, NMR, BET, FESEM, EDX and TGA. The results obtained shown that the nanomaterial synthesized is promising, as they are capable for several applications, such as Adsorption, Gas capture, Catalysis and others.

Keywords: Porous, Synthesis, Octa(aminophenyl)silesquioxane, Nanomaterial, Framework.

bonds in porous nanocrystals, which have a persistent impact on configuration geometry and porosity (Ockwig *et al.* (2005). These nanostructures are composed exclusively from light elements like, (Hydrogen, Boron, Carbon, Nitrogen, Oxygen and Silicon) (El-Kaderi *et al.* (2007). COFs are crystalline porous structures made up of organic linkers that establish reversible covalent bonds (Diercks & Yaghi (2017). The architecture of the pattern of behaviour that characterizes is determined by the size of linkers, coordination, and connectivity (Ding & Wang (2013). The conventional nanomaterials connections and spaces constituted by COFs substances are suitable for chemical conserving, liberation, and separation capabilities, while the wider and specified scaffold is beneficial for a wide range of catalysis and sensing applications. COFs are also attractive features for functionalities that require on charge carrier mobility, optoelectronics, and electrochemical power storage, among others, attributable to their regularity and binding of organic sections' interconnectivity. COFs enable "advanced" inorganic permeable crystalline materials like zeolites (Davis (2014); McCusker *et al.* (2007) and hybrid inorganic-organic metal organic frameworks (MOFs) (Burrows (2017); Lu *et al.* (2014; McCusker *et al.* (2007).

Materials and Methods

All chemicals and reagents were procured commercially and utilized without additional purification: The following chemicals were purchased from Sigma-Aldrich: octa(phenyl)silesquioxane (OPS), 1,4-dihydroxyanthraquinone (1,4-DHAQ), 1,8-dihydroxyanthraquionone (1,8-DHAQ), fuming nitric acid, tetrahydrofuran (THF), hydrazine hydrate, hexane, ethylacetate, Dimethylacetamide (DMAc), Octa(nitrophenyl)silesquioxane (ONPS) and Octa (amino phenyl)silesquioxane were produced with a moderate alteration by (Commun *et al.* (2001); Zhang *et al.* (2006).

Synthesis of Octa(nitrophenyl)silesquioxane (ONPS)

OPS, 5g (4.84 mmol), was added to a small fraction of 30 mL fuming nitric acid and agitated at 0 °C for 30 minutes before being left at room temperature for another 20 hours. The solution was placed into a 250 g ice bag and filtered through glass wool. It developed a little yellow precipitate, which was then washed with water (about 100 mL five times till pH was around 6), then rinse with ethanol (100 mL three times). To remove any remaining moisture, the powder was dried in an oven at around 80 °C. The yield powder was obtained 4g (80 %).

Synthesis of Octa (amino phenyl) silesquioxane (OAPS)

The synthesis of octa (amino phenyl) silesquioxane (OAPS) was slightly modified from that published in the literature by (Bala *et al.* (2022); Zhang *et al.* (2006). 3g of ONPS (2.60 mmol), 120 mg of $FeCl_3.6H_2O$, and 2g of activated charcoal powder were charged into a 250 mL 3 naked round-bottom bottle with a mechanical stirrer and a condenser. The flask was then supplemented with distilled THF (40 mL), under a N_2

atmosphere. The solution was agitated and heated to 60 °C, in a dropwise additions of hydrazine hydrate (13 mL) was added to the mixture. The solution was heated for 5 hours before being evacuated and filtered with celite. The filtrate was mixed with 25 mL of ethyl acetate before being washed with water. The organic layer was put into 250 mL of hexane after being dried on MgSO4. The material was redissolved in 15 mL THF and 25 mL ethyl acetate, then reprecipitated into 250 mL hexane. The powder was vacuum-dried for 24 hours. The off-white powder yields were about 40%.

Synthesis of COF-S4

OAPS (0.08 mmol, 92 mg) was mixed with 3 mL N, N'-dimethylacetamide in a 10 mL vial. The organic linker 1,5-DHAQ (C14H8O4) (0.06 mmol, 115 mg) was added to a 4mL DMAc in separate vials. The solutions were sonicated for 90 minutes at 50 °C to form a homogeneous solution, then 3-5 drops of 6M acetic acid was added. The solution was heated at 120 °C for three days, under N_2 (Bala *et al.* (2022). The result was a golden-brown powder that was washed six times with hexane 10 mL and dried under vacuum with an 80 mg yield.

Results and Discussion

We designed two new COFs COF-S4 via solvothermal process with OAPS as central molecule with 1,4-DHAQ as organic linker, as shown in scheme 1.

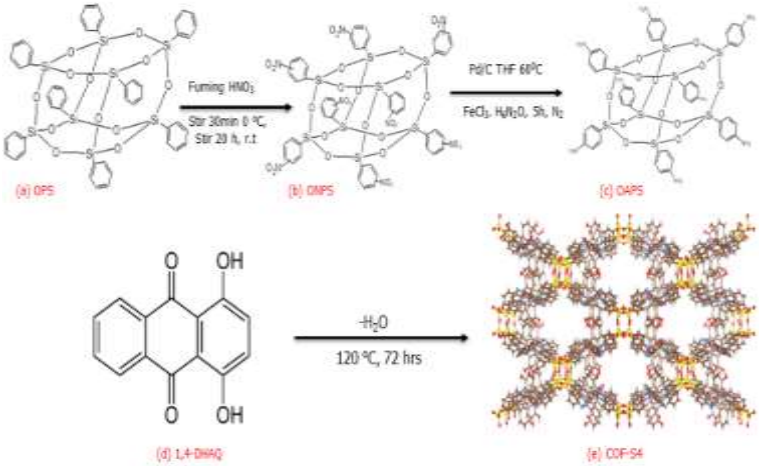

Scheme 1.

Nitration of a yields b, and reduction to produce c. Condensation of (c & d) and (c & e) lead to the production of (molecular units) which will join together the tetrahedral building blocks D and E to produce the diamond like structures of POSS (f) COF-S4 and (g) COF-S14, single framework (space filling, Carbon =brown, Oxygen =red, Nitrogen= blue and Silicone = yellow) Hydrogens were omitted for clarity.

Powder X-Ray Diffraction (PXRD)

The synthesized COF-S4 materials was characterized using PXRD, (solid ^{13}C and ^{29}Si). The PXRD pattern of COF-S4 compound shown in Figure 1, corresponding with the simulated pattern, validating that the nanomaterials were effectively produced and their chemical stability structures persisted unaffected after dissolving in a number of protic and aprotic solvents for 24 hours.

The compound synthesized exhibited important strong peaks at below 10 degrees (< 10). COF-S4 observed 2θ signals at 8.4, 9.8, 10.4, 21.73 and 24.74º which accorded to various hump-ordered reflections (110), (112), (12-5), (224) and (316) planes. (431), (512) and (406) reflections, respectively. The arrays from the intensity of the simulated and as-synthesized COF might be owing to the non-full connectivity amid the central composite (OAPS) and the organic linker, consequently, the occurrence of the products from the partial reaction might be existing in the materials attained (Bala *et al*. (2022). Table 1, shows the crystallographic and structural data of the synthesized COF.

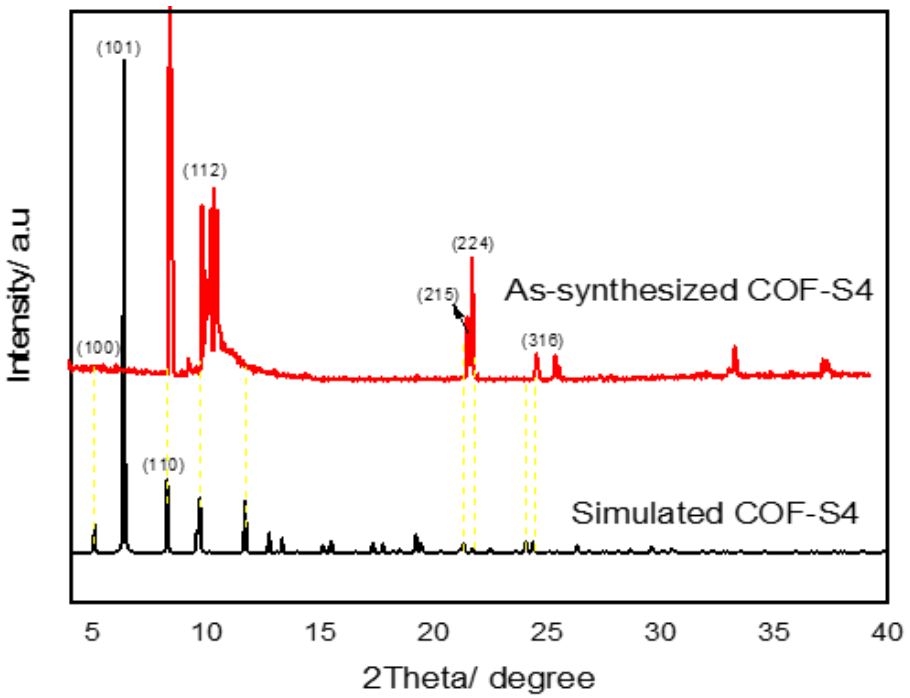

Figure 1. PXRD spectra of as-synthesized and simulated of (a) COF-S4

Table 1: Crystallographic and structural data of calculated COF-S4

Compound	COF-S4
Empirical formular	$C_{21}H_{16}N_2O_5Si_2$
Formular weight g/mol	1730.14
Crystal system	Tetragonal
Space group	I-4
Unit cell dimension /Å	*a*=15.147, *b*=15.147, *c*=34.979
α, β, γ /° Volume /Å³	90, 90, 90 8025.5
Z, (No. of atom/unit cell	8
Calculated density, (ρ) g/cm^{-3}	0.7160
Theta range for data collection /º	3.0 - 45.0

Fourier Transform Infrared Spectroscopy (FTIR)

The ONPS was produced and its structure was analyzed. In the FTIR spectra of ONPS, the two strong peaks at 1344 and 1537 cm^{-1} were ascribed to symmetry and asymmetry υN=O, respectively. The two strong absorption bands fell after reduction with hydrazine hydrate, which functioned as a reducing agent as revealed in the FTIR spectra of OAPS, demonstrating that the reduction process was attained. Furthermore, new broad peaks were observed in the OAPS spectra at 3352 and 3224 cm^{-1}, which were attributed to primary imine υN-H Stretching. Similar investigation found that the symmetry and asymmetry of N=O were identified at 1350 cm^{-1} and 1529 cm^{-1}, respectively. Stretching of υN-H bonds was also discovered at 3369 cm^{-1} and 3220 cm^{-1}, respectively (Bala *et al.* (2022); Zhang *et al.* (2006). In the FTIR Spectrum of the OAPS, the Si-O-Si interaction was observed at 1092 cm^{-1} with a minor decrease in the ONPS molecule appeared at 1074 cm^{-1}. The Si-O-Si bonds for the ONPS and OAPS were observed at 1119 cm^{-1} and 1100 cm^{-1}, respectively,

Figure 2. The υC=N bonds observed as a result of the interactions involving OAPS and linkers for the azomethine group (Schiff base reaction) is the most defining property of all the material produced. υC=N bond for the COF-S4 as shown in Fig. 2, was observed at the frequencies of 1593 cm^{-1} and 1503 cm^{-1}, respectively. From the absorption bands demonstrated, the coordination reaction from the OAPS nitrogen atom and the linkers carbon atom was effective. Similar research was published in 2017 for imine-based COFs, in which C=N interactions were formed at a frequency of 1621 cm^{-1}. (Matsumoto *et al.* (2017; Vitaku & Dichtel (2017); Wan *et al.* (2011). Broad peaks were identified at 3176 cm^{-1} in COF-S4 which was attributed to the O-H unit,

which may have originated from 1,4-DHAQ linker, respectively. This result is consistent with . (Clark (2019) a previously published report on broad bonding of O-H absorption spectra in the 2500-3300 cm^{-1} regions

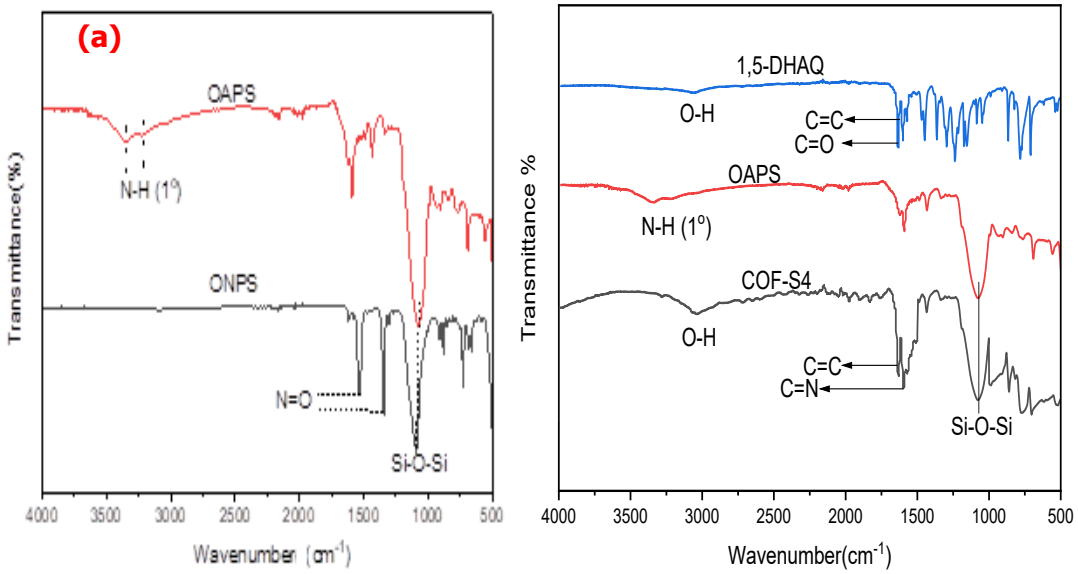

Figure 2: FTIR spectra of (a) ONPS (black), OAPS (red) (b) COF-S4(black) OAPS (red), 1,5-DHAQ (blue).

Nuclear Magnetic Resonance Spectroscopy (NMR)

^{1}H-NMR Spectra of ONPS and OAPS

The ^{1}H NMR spectra of the ONPS and OAPS in deuterium acetone (acetone-d6) were analysed to determine the synthesis of the new material (Figure 3). The aromatic hydrogens of OAPS were discovered at a larger chemical shift (7.47 – 6.34 ppm) due to the electron donor features of amino groups (NH_2) on phenyl rings, those for the amino protons were observed in the lower region at 4.0-5.0 ppm. The synthesis was supported by a study documented by (Bala *et al.* (2022; Jothibasu

et al. (2008). Due to the electro-withdrawing activities of nitro groups (NO_2) on the aromatic rings of the ONPS, the signals corresponding to aromatic hydrogen protons were observed in the range of ONPS at lower chemical shift (8.7 -7.8 ppm). Additional aromatic peaks can be found in the ONPS region, including triplet peaks at (8.67 ppm) that are assumed to be protons between the nitro (NO_2) and siloxy (Si-O-Si) groups in the meta isomer. The meta and para ratios were estimated to be 52 percent and 48 percent, respectively, given that the ortho is negligible. Specific studies found that the ONPS peaks were found at 8.7-7.8 ppm, whereas the spectrum of OAPS was found at 7.8 - 6.2 ppm and 7.8 - 6.0 ppm, respectively(Commun *et al*. (2001); Yang *et al*. (2010).

CP-MAS ^{13}C Solid state NMR Spectrum of OAPS

The ^{13}C-NMR supported the synthesis, as evidenced from the ONPS-assigned patterns were totally replaced by new OAPS cluster signals in the higher region 118.0 – 152.9 ppm (Figure 3). Distinct aromatic carbon environments peaks were found at 118.05, 132.39, 147.27, and 152.93 ppm, respectively. This demonstrates that the cage architecture of polyhedral Oligosilsesquioxane remains stable after synthesis. The same synthesis were confirmed by (Commun *et al*. (2001); Qin *et al*. (2013).

CP-MAS ^{29}Si solid state NMR of OAPS

The robustness of the oligomeric silesquioxane cage structure in the synthesis was further validated using the Si solid state NMR spectra for OAPS. The acquired results clearly demonstrated that the cage geometry of the polyhedral silesquioxane is conserved throughout synthesis, as shown in Figure 3, with OAPS peak positions of -79 and -69.6 ppm. This

is consistent with established research investigations conducted using a conventional technique by (Bala *et al.* (2022); Commun *et al.* (2001); Ni & Zheng (2004); Zhang *et al.* (2006).

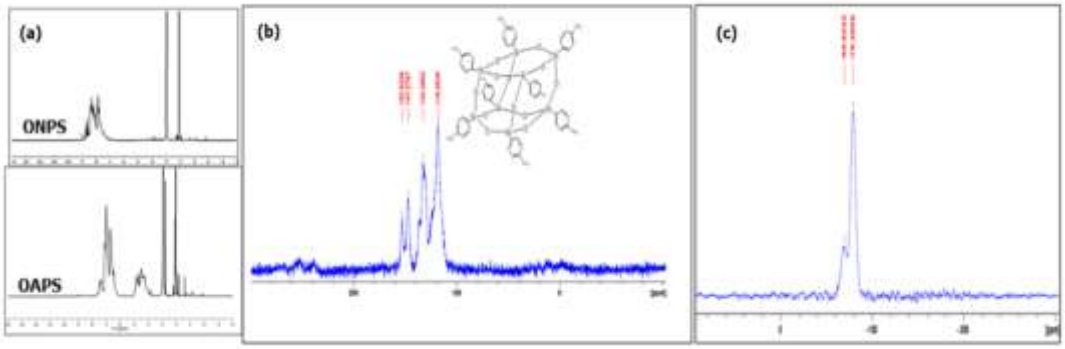

Figure 3: 1H-NMR spectra of (a) ONPS and OAPS, (b) CP-MAS 13C spectra of OAPS and (c) 29Si spectra of OAPS

CP-MAS ^{13}C and ^{29}Si NMR spectra of COF-S4

The ^{13}C-NMR spectra for the COFs developed as presented in Figure 4a, shown a diverse carbon environs for the linkers and the OAPS. In COF-S4. The resonance ranges were investigated at the signals 117.03–136.8 ppm were assigned to aromatic carbons (phenyl rings) for OAPS cluster and a linker present in the formulation of the nanomaterials (Das *et al.* (2014). By comparing the signals of OAPS and the COF synthesized, the corresponding chemical shifts were slightly shifted to lower chemical shifts owing to the influence of the aromatic linker. A similar study conducted by Hoffman and colleagues reported are in agreement (Hoffmann *et al.* (2012). Similarly, the synthesized COFs revealed the chemical shifts of the azomethine carbons (C=N) at a resonance of 162.05 ppm. Same studies were documented (Das *et al.* (2014); Hoffmann *et al.* (2012). Asterisks denotes spinning side-banned signals

which are phantom signs (i.e., peaks) caused by the magnetic force amplification at the twirling frequency. The peaks typically emerge at a level equivalent to the spinning velocity on each side of any significant actual peak.

Solid state ^{29}Si MAS CP-NMR was further used to evaluate the synthesis of the novel material by revealing the existence of silicon in the cubic silesquioxane. The findings acquired proved the effectiveness in the synthesis of the COFs as shown in Figure 4b. The magic angle spinning conferred had one single signal for each COF with a chemical shift of -83.57 ppm. These results identified the Si8 vertices throughout the COF structure. The orientation of the cubic silesquioxane vertices from the starting material OAPS was all at the identical positions, allowing for the detection of a single chemical shifts. Related studies on the synthesis of COFs material containing silicone are in agreement with this study (Bala *et al.* (2022); Hunt *et al.* (2008); Yahiaoui *et al.* (2018) This analysis further confirmed the rigidity and consistency of the cage frameworks even after the synthesis of COFs.

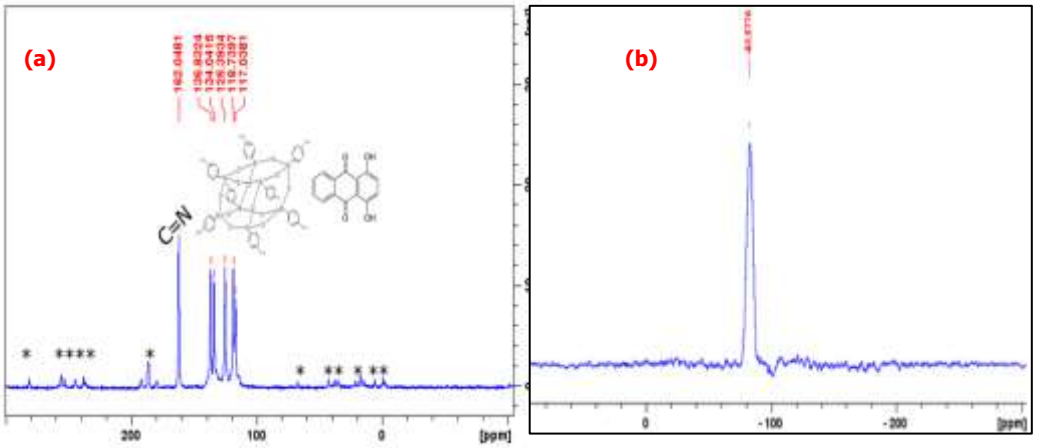

Figure 4: CP-MAS ^{13}C and ^{29}Si -NMR spectrum of COF-S4

Thermogravimetric Analysis (TGA)

TGA investigation of as-synthesised COF-S4 material were accomplished under oxygen at temperatures ranging from 50 to 800 ºC min^{-1} and a thermal rate of 10 ºC min^{-1} (Figure 5a). The as-synthesised nanomaterial was initially submerged in a high boiling point liquid (DMAc) for a sufficient period prior to the analyses to enable liquid dispersion into the pores. The COF was therefore processed rapidly to eliminate any solvent molecules that had not become entrapped in the pores (Chen *et al.* (2019; Howarth *et al.* (2017). The as-synthesised COF-S4 displayed a mass loss of 5.2 wt.% at the range of 50 — 150 °C accredited to the loss of water molecules. The mass loss of 14.6 wt.% at 150 to 250 °C was designated to the disintegration of unwanted diluent, dimethylacetamide (DMAc). The structure began to disintegrate progressively at about 300 °C (Bala *et al.* (2022); Gropp *et al.* (2020); Nguyen *et al.* (2020) reflecting to the depletion of linker (1,4-DHAQ), and OAPS frameworks with mass loss of about 61.61 wt.%.

Field Emission scanning electron microscopy (FESEM)

FESEM is a technique use to view the morphological structure and crystal size of the material. The analysis was conducted on COF-S4, at a (magnifications,50 and 100) an accelerating voltage of 5.0 Kv electron beam was used during the analysis to obtain a good image resolution and the materials were dispersed over a sticky carbon surface adhered to a flat platinum platform sample holder as depicted in Figure 5b. COF-S4, displayed a dense cloudier silica particle with morphological nano pores, with 1 µm. A similar surface structure was reported (Roeser *et al.* (2017), where a SiCOF-Li and SiCOF-Na were synthesized from silica

gel and tetramethyl orthosilicate, with 9,10- Dimethyl-2,3,6,7-tetrahydroxyanthracene as linker.

Energy Dispersive X-Ray Analysis (EDX)

The elemental composition of solid surfaces or materials can be determined using energy-dispersive X-ray spectroscopy (EDX). It's also a method for identifying the elemental composition of numerous different components of a substance. It is based on an interface between an X-ray emitter and a probe. Its characterisation powers are largely attributable to the basic credence that each component has a distinct arrangement of atoms, resulting in a distinct collection of spots on its electromagnetic spectral lines. COFs were disseminated over adhesive carbon surface held to a flat platinum platform sample holder and popped in an argon environment. In this study, the EDX was used to confirmed the elemental constituents (%) and other impurities. COF-S4, spectra (a), displayed atomic peaks that proved the presence of elements (C, N, O and Si) in percentages, which further confirmed the synthesis of the novel COFs. COF-S4 is ascribed with the atomic % of 55.44, 13.88, 25.95, 4.73 and weight % of 60.57, 6.71, 19.21, 13.48 for C, N, O, and Si atoms, respectively, owing to their uniform atomic composition. This result is in close to argument with previous research reported (Roeser *et al.* (2017); Zhang *et al.* (2020).

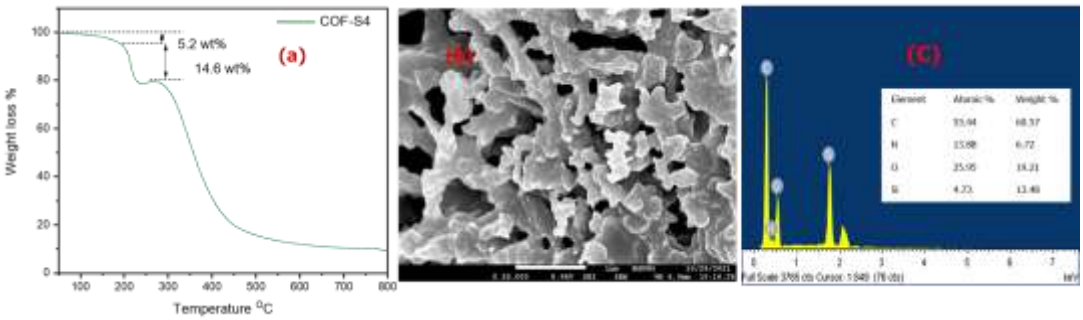

Figure 5: (a) TGA thermogram of COF-S4 at heating rate of 10 °C min^{-1} under oxygen flow, (b): FESEM images of COF-S4 (a and b), at 50x under 5.0 kV accelerating voltage and (c) EDX spectra and weight percentages of identified elements.

N_2 Physisorption analysis

This approach depicts the physical adsorption of gas molecules on a solid surface (Karozis *et al.* (2017). It gives a crucial information about the materials that Langmuir, Freundlich, and Brunauer-Emmett-Teller (BET) concept can interpret. By analysing the surface area inside the pore structure. Prior to the analysis, COF-S4, was activated by solvent-exchange and oven-dried at 100 °C over night to remove all the guest molecules. Figure 6. Table 2. presented the summary of surface area and pore opening data were reported accordingly. The as-synthesized sample was used for measurement of the isotherm at 77 K from 0 to 1 bar (1 bar = P_o), which shown that the COF unveiled a Type IV isotherm which demonstrated a distinctive of mesoporous materials with pore size of lower than 50 nm. The hysteresis loops are known as the capillary condensation that occurs in a mesopores with regulated uptake of high P/P_o lower than 1. The as-synthesized COF from the adsorption isotherm indicated Type H3 hysteresis loops in the range of 0.5-0.9 relative pressure. P/P_o which implied an extensive dispersal in pore size (Renzo *et al.* (2009). A type IV with a hysteresis loop was revealed in a comparable study, which was described by a rapid absorption under low relative pressures at P/P_o 0.01 followed by a second step in 0.05 P/P_O 0.20, which is evocative of a mesoporous structure (Zeng *et al.* (2015).

COF-S4 possessed a BET surface area of 5.14, m^2g^{-1}. The low surface area adsorption was most likely due to surface tension that occurred during the activation of the COF as the low boiling point solvent utilized is likely to possess strosng hydrogen bonding to the vertices of COFs. These

diluents will breed adequate capillary strength that lead to the fractional or whole interference of COFs scaffolds or very low N_2 uptake and trivial surface area could be owed to the blockage of the pore networks by enormous fragments (Ayoub *et al.* (2019); Bala *et al.* (2022); Zeng *et al.* (2015) This could be owing to the alcohol group's (OH) strong polarity and hydrogen capacity, which makes COF activation difficult. As a result, supercritical CO_2 adsorption activation drying should be an attractive potential activation strategy to alleviate surface tension and inhibit pore decline upon expulsion of solvent, as demonstrated in the case of IRMOF-3 activation using this approach, which yielded a large specific surface area of 2850 m^2g^{-1} compares favourably to solvent-exchange activation (DMF↔$CHCl_3$), which yielded 1800 m^2g^{-1} (Nelson *et al.* (2009).

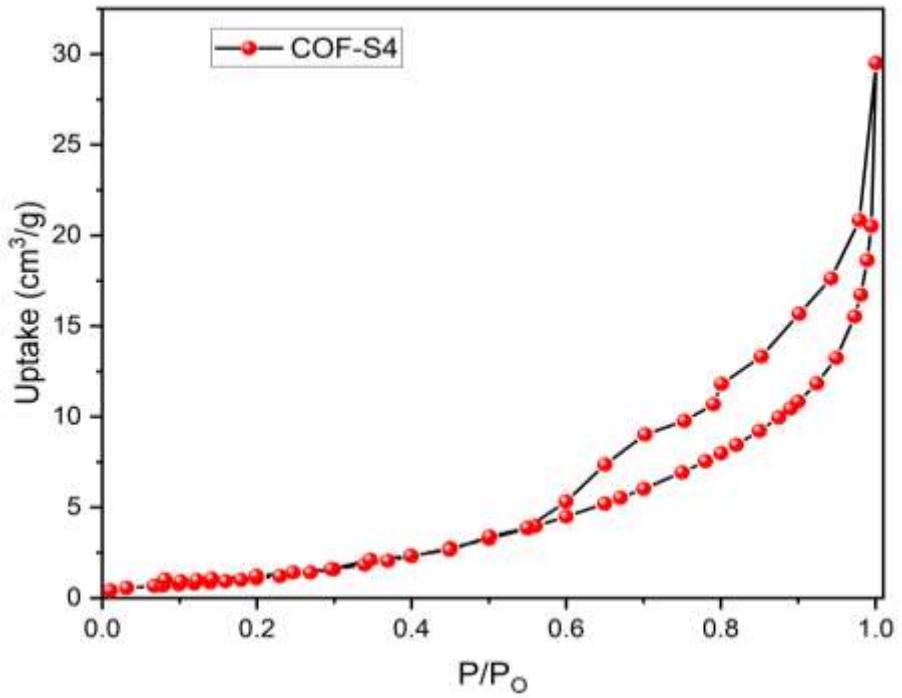

Figure 6: N_2 isotherm of COF-S4, at 77K

Table 2: Summary of the surface area and pore opening data of COF-S4

Compound	COF-S4
Theoretical surface area/ m^2/g	5095.60
Experimental surface area/ m^2/g	5.14
Theoretical pore opening	
Large/Å	11.52
Small/Å	11.49
Experimental pore opening (4V/A by BET)	
Adsorption/Å	4.95
Desorption/Å	140.99
BJH average pore width (4V/A)	
Adsorption/Å	54.15
Desorption/Å	53.78

Conclusion

The COF synthesized demonstrated eight connected octahedral nets from the eight nitrogen atoms from the OAPS assembly. Interestingly, the material synthesized displayed a new topology with a 2D underlayer arrangement that was not predictable before using the Reticular Chemistry Structure Resource (RCSR). The analysis done further proven the successes recorded and rigidness of the structure of the compound. A UV/spectroscopy system was used to study the adsorption of naproxen on the adsorbents A significant number of adsorbates were eliminated after 270 min. As a result of this extensive assembling and adsorption recyclability study, POSS COFs may be employed with impressive results in the future for the adsorption treatment of pharmaceutical waste.

Acknowledgement: I thank the TETFUND Institution-based research (IBR) Intervention Allocation and the Management of the Federal Polytechnic Mubi, Adamawa State for funding this Research Work.

Disclosure statement: ***Conflict of Interest:*** The authors declare that there are no conflicts of interest.

References:

Ayoub, G., Islamoglu, T., Goswami, S., Friščić, T., & Farha, O. K. (2019). Torsion Angle Effect on the Activation of UiO Metal-Organic Frameworks. *ACS Applied Materials and Interfaces*, *11*(17), 15788–15794. https://doi.org/10.1021/acsami.9b02764

Bala, S., Abdullah, C. A. C., Tahir, M. I. M., & Abdul Rahman, M. B. (2022). Adsorptive Removal of Naproxen from Water Using Polyhedral Oligomeric Silesquioxane (POSS) Covalent Organic Frameworks (COFs). *Nanomaterials*, *12*(14), 2491. https://doi.org/10.3390/nano12142491

Burrows, A. D. (2017). The Chemistry of Metal–Organic Frameworks. Synthesis, Characterization, and Applications, 2 Volumes. Edited by Stefan Kaskel. *Angewandte Chemie International Edition*, *56*(6), 1449–1449. https://doi.org/10.1002/anie.201611669

Chen, Yichong, Shi, Z. L., Wei, L., Zhou, B., Tan, J., Zhou, H. L., & Zhang, Y. B. (2019). Guest-Dependent Dynamics in a 3D Covalent Organic Framework. *Journal of the American Chemical Society*. https://doi.org/10.1021/jacs.8b13691

Clark, J. (2019). Identifying the Presence of Particular Groups. *Libretexts*, 1–3. https://chem.libretexts.org/Bookshelves/Physical_and_Theoretical_Chemistry_Textbook_Maps/Supplemental_Modules_(Physical_and_Theoretical_Chemistry)/Spectroscopy/Vibrational_Spectroscopy/Infrared_Spectroscopy/Identifying_the_Presence_of_Particular_Groups

Commun, K. D. C., Tamaki, R., Tanaka, Y., Asuncion, M. Z., Choi, J., Laine, R. M., & July, R. V. (2001). *A key problem with almost all of the materials explored to date is that the aliphatic components limit the thermal stability of the resulting nanocomposites , strongly influence (lower) T g , and decrease mechanical properties potentials . Hence we soug*. *15*, 12416–12417.

Cuerda-Correa, E. M., Domínguez-Vargas, J. R., Olivares-Marín, F. J., & de Heredia, J. B. (2010). On the use of carbon blacks as potential low-cost adsorbents for the removal of non-steroidal anti-inflammatory drugs from river water. *Journal of Hazardous Materials*, *177*(1–3), 1046–1053. https://doi.org/10.1016/j.jhazmat.2010.01.026

Das, G., Balaji Shinde, D., Kandambeth, S., Biswal, B. P., & Banerjee, R. (2014). Mechanosynthesis of imine, β-ketoenamine, and hydrogen-bonded imine-linked covalent organic frameworks using liquid-assisted grinding. *Chemical Communications*, *50*(84), 12615–12618. https://doi.org/10.1039/c4cc03389b

Davis, M. E. (2014). ChemInform Abstract: Zeolites from a Materials Chemistry Perspective. *ChemInform*, *45*(10), no-no. https://doi.org/10.1002/chin.201410237

Diercks, C. S., & Yaghi, O. M. (2017). The atom, the molecule, and the covalent organic framework. *Science*, *355*(6328). https://doi.org/10.1126/science.aal1585

Ding, S. Y., & Wang, W. (2013). Covalent organic frameworks (COFs): From design to applications. *Chemical Society Reviews*, *42*(2), 548–568. https://doi.org/10.1039/c2cs35072f

El-Kaderi, H. M., Hunt, J. R., Mendoza-Cortés, J. L., Côté, A. P., Taylor, R. E., O'Keeffe, M., & Yaghi, O. M. (2007). Designed synthesis of 3D covalent organic frameworks. *Science*, *316*(5822), 268–272. https://doi.org/10.1126/science.1139915

Gropp, C., Canossa, S., Wuttke, S., Gándara, F., Li, Q., Gagliardi, L., & Yaghi, O. M. (2020). Standard Practices of Reticular Chemistry. *ACS Central Science*, *6*(8), 1255–1273. https://doi.org/10.1021/acscentsci.0c00592

Hoffmann, H. C., Debowski, M., Müller, P., Paasch, S., Senkovska, I., Kaskel, S., & Brunner, E. (2012). Solid-state NMR spectroscopy of metal-organic framework compounds (MOFs). *Materials*, *5*(12), 2537–2572. https://doi.org/10.3390/ma5122537

Howarth, A. J., Peters, A. W., Vermeulen, N. A., Wang, T. C., Hupp, J. T., & Farha, O. K. (2017). Best practices for the synthesis, activation, and characterization of metal—organic frameworks. *Chemistry of Materials*, *29*(1), 26–39. https://doi.org/10.1021/acs.chemmater.6b02626

Hunt, J. R., Doonan, C. J., LeVangie, J. D., Côté, A. P., & Yaghi, O. M. (2008). Reticular synthesis of covalent organic borosilicate frameworks. *Journal of the American Chemical Society*, *130*(36), 11872–11873. https://doi.org/10.1021/ja805064f

Jothibasu, S., Premkumar, S., Alagar, M., & Hamerton, I. (2008). Synthesis and characterization of a POSS-maleimide precursor for hybrid nanocomposites. *High Performance Polymers*, *20*(1), 67–85. https://doi.org/10.1177/0954008307079541

Karozis, S., Charalambopoulou, G., Steriotis, T., Stubos, A., & Kainourgiakis, M. (2017). Colloids and Surfaces A : Physicochemical and Engineering Aspects Determining the specific surface area of Metal Organic Frameworks based on a computational approach. *Colloids and Surfaces A: Physicochemical and Engineering Aspects*, *526*, 14–19. https://doi.org/10.1016/j.colsurfa.2016.12.016

Lu, W., Wei, Z., Gu, Z. Y., Liu, T. F., Park, J., Park, J., Tian, J., Zhang, M., Zhang, Q., Gentle, T., Bosch, M., & Zhou, H. C. (2014). Tuning the structure and function of metal-organic frameworks via linker design. *Chemical Society Reviews*, *43*(16), 5561–5593. https://doi.org/10.1039/c4cs00003j

Matsumoto, M., Dasari, R. R., Ji, W., Feriante, C. H., Parker, T. C., Marder, S. R., & Dichtel, W. R. (2017). Rapid, Low Temperature Formation of Imine-Linked Covalent Organic Frameworks Catalyzed by Metal Triflates. *Journal of the American Chemical Society*, *139*(14), 4999–5002. https://doi.org/10.1021/jacs.7b01240

McCusker, L. B., Olson, D. H., & Baerlocher, C. (2007). Atlas of Zeolite Framework Types. In *Atlas of Zeolite Framework Types*. https://doi.org/10.1016/B978-0-444-53064-6.X5186-X

Nelson, A. P., Farha, O. K., Mulfort, K. L., & Hupp, J. T. (2009). *Supercritical Processing as a Route to High Internal Surface Areas and Permanent Microporosity in Metal - Organic Framework Materials*. *D*, 458–460.

Nguyen, H. L., Gropp, C., & Yaghi, O. M. (2020). Reticulating 1D Ribbons into 2D Covalent Organic Frameworks by Imine and Imide Linkages. *Journal of the American Chemical Society*, *142*(6), 2771–2776. https://doi.org/10.1021/jacs.9b13971

Ni, Y., & Zheng, S. (2004). A novel photocrosslinkable polyhedral oligomeric silsesquioxane and its nanocomposites with poly(vinyl cinnamate). *Chemistry of Materials*, *16*(24), 5141–5148. https://doi.org/10.1021/cm049463k

Ockwig, N. W., Co, A. P., Keeffe, M. O., Matzger, A. J., & Yaghi, O. M. (2005). *Porous , Crystalline , Covalent Organic Frameworks*. *310*(November), 1166–1171.

Qin, Y., Peng, Q., & Song, J. (2013). Preparation of polyhedral oligosilsesquioxane-based organic-inorganic hybrid porous nanocomposite by freeze-drying conditions. *Asian Journal of Chemistry*, *25*(3), 1229–1232. https://doi.org/10.14233/ajchem.2013.12609

Renzo, F. Di, Chang, S., Clair, B., Ruelle, J., & Beauche, J. (2009). *Mesoporosity as a new parameter for understanding tension stress generation in trees*. *60*(11), 3023–3030. https://doi.org/10.1093/jxb/erp133

Roeser, J., Prill, D., Bojdys, M. J., Fayon, P., Trewin, A., Fitch, A. N., Schmidt, M. U., & Thomas, A. (2017). Anionic silicate organic frameworks constructed from hexacoordinate silicon centres. *Nature Chemistry*, *9*(10), 977–982. https://doi.org/10.1038/nchem.2771

Vitaku, E., & Dichtel, W. R. (2017). Synthesis of 2D Imine-Linked Covalent Organic Frameworks through Formal Transimination Reactions. *Journal of the American Chemical Society*, *139*(37), 12911–12914. https://doi.org/10.1021/jacs.7b06913

Wan, S., Gándara, F., Asano, A., Furukawa, H., Saeki, A., Dey, S. K., Liao, L., Ambrogio, M. W., Botros, Y. Y., Duan, X., Seki, S., Stoddart, J. F., & Yaghi, O. M. (2011). Covalent organic frameworks with high charge carrier mobility. *Chemistry of Materials*, *23*(18), 4094–4097. https://doi.org/10.1021/cm201140r

Yahiaoui, O., Fitch, A. N., Hoffmann, F., Fröba, M., Thomas, A., & Roeser, J. (2018). 3D anionic silicate covalent organic framework with srs topology. *Journal of the American Chemical Society*, *140*(16), 5330–5333. https://doi.org/10.1021/jacs.8b01774

Yang, Z., Peng, H., Wang, W., & Liu, T. (2010). Crystallization behavior of poly(ε-caprolactone)/layered double hydroxide nanocomposites. *Journal of Applied Polymer Science*, *116*(5), 2658–2667. https://doi.org/10.1002/app

Zeng, Y., Zou, R., Luo, Z., Zhang, H., Yao, X., Zou, R., & Zhao, Y. (2015). *Covalent Organic Frameworks Formed with Two Types of Covalent Bonds Based on Orthogonal Reactions*. 1021–1024. https://doi.org/10.1021/ja510926w

Zhang, J., Xu, R., Yu, D., & Si, À. (2006). *A Novel and Facile Method for the Synthesis of Octa (aminophenyl) silsesquioxane and Its Nanocomposites with Bismaleimide-Diamine Resin*. https://doi.org/10.1002/app

Zhang, Y., Yuan, X., Jiang, W., & Liu, H. (2020). Determination of nereistoxin-related insecticide via quantum-dots-doped covalent organic frameworks in a molecularly imprinted network. *Microchimica Acta*, *187*(8). https://doi.org/10.1007/s00604-020-04435-z

03.31.2024

JOURNAL OF

Health, Metabolism & Nutrition Studies (JHMNS) Vol. 3 No. 3

MEDICAL AND PHARMACOLOGICAL PROPERTIES OF *OCIMUM GRATISSIMUM* (SCENT LEAF): A REVIEW

OKOYE, C. I.; ADAMU, B. B.; ABUBAKAR, Z. I.; IDRIS, H. A.; MAIDAWA, G. L; MUSTAPHA, F. A.; AYEGBA, S. O.; & ABDALLAH, H.Y.

National Biotechnology Development Agency, Abuja, Nigeria.

Abstract

Ocimum gratissimum is a well-known plant used in the Indian system of medicine. Folklore medicine claims its use in headache, fever, diarrhoea, pneumonia etc. Research carried out using different *in vitro* and *in vivo* techniques of biological evaluation supports most of the claims.The ethanolic extract of the leaves of *Ocimium gratisimum* L. (Lamiaceae), used in traditional medicine for the treatment of several ailments such as urinary tract, wound, skin and gastrointestinal infections, was evaluated for its antibacterial properties against four clinical bacteria isolates namely: *Escherichia coli, Proteus*

Introduction

Ocimum gratissimum, also known as clove basil, African basil, and in Hawaii as wild basil, is a species of Ocimum. It is native to Africa, Madagascar, southern Asia, and the Bismarck Archipelago, and naturalized in Polynesia, Hawaii, Mexico, Panama, West Indies, Brazil, and Bolivia (Mann *et al.,* 2019). *Ocimum gratissimum* is an aromatic herb that been

E-ISSN 3026-8664 P-ISSN3027-2238

mirabilis, Staphylococcus aureus and Pseudomonas aeruginosa and the antifungal properties using a clinical isolate of *Candida albicans*. This review paper presents the ethnobotanical, natural product chemistry, pharmacological, clinical information of the plant.

Key words: *Ocimum gratissimum* Pharmacological Extract Plant

Introduced extensively across tropical and subtropical regions of the world. It has escaped cultivation and can be found growing as a weed in disturbed sites, waste areas, pastures and along roadsides, but also invading disturbed natural vegetation, savannas, coastal thickets and riparian areas. In this species, seeds are small and numerous and easily dispersed by gravity, animals, human activities and as a contaminant in soil and garden debris (Aziba *et al.,* 2019). Once established, *O. gratissimum* has the potential to grow forming dense monospecific thickets that outcompete native vegetation and reduce native biodiversity (Okwu *et al.,* 2018).

Ocimum gratissimum L. is a medicinal plant widely grown in tropical and subtropical regions with the leaf decoction usually taken in folk medicine to enhance erectile performance in men although the probable mechanism of actions remains undetermined (Kalita *et al.,* 2019).

Origin of *Ocimum gratissimum*

Ocimum gratissimum, also known as clove basil, African basil, and in Hawaii as wild basil, is a species of *Ocimum*. It is native to Africa, Madagascar, southern Asia, and the Bismarck Archipelago, and naturalized in Polynesia, Hawaii, Mexico, Panama, West Indies, Brazil, and Bolivia *O. gratissimum* is found throughout the